

1 **Monoterpene chemical speciation in a tropical rainforest: variation with season, height, and time**  
2 **of day at the Amazon Tall Tower Observatory (ATTO)**

3 **Ana María Yáñez-Serrano<sup>1,\*</sup>, Anke Christine Nölscher<sup>1,\*\*</sup>, Efstratios Bourtsoukidis<sup>1</sup>, Eliane Gomes**  
4 **Alves<sup>2</sup>, Laurens Ganzeveld<sup>3</sup>, Boris Bonn<sup>4</sup>, Stefan Wolff<sup>1</sup>, Marta Sa<sup>2</sup>, Marcia Yamasoe<sup>5</sup>, Jonathan**  
5 **Williams<sup>1</sup>, Meinrat O. Andreae<sup>1,6</sup> and Jürgen Kesselmeier<sup>1</sup>**

6 [1] {Air Chemistry, Biogeochemistry and Multiphase Departments, Max Planck Institute for Chemistry,  
7 D-55020 Mainz, Germany}

8 [2] {Instituto Nacional de Pesquisas da Amazônia (INPA), Av. André Araújo 2936, Manaus-AM, Brazil}

9 [3] {Meteorology and Air Quality (MAQ), Department of Environmental Sciences, Wageningen Univer-  
10 sity and Research Centre, Wageningen, the Netherlands}

11 [4] {Chair of Tree Physiology, Albert Ludwig University, Freiburg, Germany}

12 [5] {Instituto de Astronomia, Geofísica e Ciências Atmosféricas, Universidade de São Paulo, Rua do  
13 Matão 122, São Paulo-SP, Brazil}

14 [6] {Scripps Institution of Oceanography, University of California San Diego, La Jolla, CA, USA}

15 \* Now at Chair of Ecosystem Physiology, Albert Ludwig University, Freiburg, Germany.

16 \*\* Now at German Weather Service, Offenbach am Main, Germany.

17  
18 Correspondence e-mail: a.yanezserrano@mpic.de

19  
20 Speciated monoterpene measurements in rainforest air are scarce, but they are essential for understand-  
21 ing the contribution of these compounds to the overall reactivity of volatile organic compound (VOCs)  
22 emissions towards the main atmospheric oxidants, such as hydroxyl radical (OH), ozone (O<sub>3</sub>) and ni-  
23 trate radical (NO<sub>3</sub>). In this study, we present the chemical speciation of gas phase monoterpenes meas-  
24 ured in the tropical rainforest at the Amazon Tall Tower Observatory (ATTO, Amazonas, Brazil). Sam-  
25 ples of VOCs were collected by two automated sampling systems positioned on a tower at 12 and 24 m  
26 height and analysed using Gas Chromatography Flame Ionization Detection (GC-FID). The samples  
27 were collected in October 2015, representing the dry season, and compared with previous wet and dry  
28 season studies at the site. In addition, vertical profile measurements (at 12 and 24 m) of total monoter-  
29 pene mixing ratios were made using Proton-Transfer Reaction Mass Spectrometry (PTR-MS). The re-  
30 sults showed a distinctly different chemical speciation between day and night. For instance,  $\alpha$ -pinene  
31 was more abundant during the day, whereas limonene was more abundant at night. Reactivity calcula-  
32 tions showed that higher abundance does not generally imply higher reactivity. Furthermore, inter- and  
33 intra-annual results demonstrate similar chemodiversity during the dry seasons analysed. Simulations  
34 with a canopy exchange modelling system show simulated monoterpene mixing ratios that compare rel-  
35 atively well with the observed mixing ratios, but also indicate the necessity of more experiments to en-  
36 hance our understanding of in-canopy sinks of these compounds.

37

38 **1. Introduction**

39 Isoprenoids such as isoprene ( $C_5H_8$ ), monoterpenes ( $C_{10}H_{16}$ ) and sesquiterpenes ( $C_{15}H_{24}$ ) are  
40 considered to be key contributors to the production of biogenic secondary organic aerosol (SOA), which  
41 affects cloud condensation nuclei production (Engelhart et al., 2008; Jokinen et al., 2015; Pöschl et al.,  
42 2010). While isoprene is a globally significant source of SOA (Claeys et al., 2004), its presence can also  
43 inhibit SOA formation under certain conditions (Kiendler-Scharr et al., 2009). By virtue of their lower  
44 volatility and higher ozone reactivity, monoterpenes and sesquiterpenes are strong sources of secondary  
45 organic aerosol (SOA) through the generation of low-volatility oxidation products formed via ozonoly-  
46 sis and hydroxyl radical oxidation (Bonn and Moortgat, 2003; Zhao et al., 2015).

47  
48 The main source of monoterpenes to the global atmosphere is emission from vegetation, with  
49 smaller contributions from soil (Kesselmeier and Staudt, 1999; Kuhn et al., 2002; Ormeno et al., 2007).  
50 Synthesis of the monoterpene species occurs via the non-mevalonate pathway within the plant chloro-  
51 plast (Kesselmeier and Staudt, 1999; Lichtenthaler, 1999; Schwender et al., 1996), which explains the  
52 light dependency also known to determine isoprene synthesis and emission. These commonly emitted  
53 compounds have been identified as important signalling compounds through plant-to-plant, plant-insect  
54 or plant-microbe interactions (Gershenzon, 2007; Gershenzon and Dudareva, 2007; Kishimoto et al.,  
55 2006; Maag et al., 2015) and they are thought to protect photosynthetic membranes against abiotic  
56 stresses (Jardine et al., 2017; Penuelas and Llusia, 2002; Vickers et al., 2009).

57  
58 Despite having a common sum formula, variations in the molecular structure of the various  
59 monoterpenes result in large variations (over two orders of magnitude) of their reaction rate coefficients  
60 with the hydroxyl radical (OH), ozone ( $O_3$ ) and nitrate radical ( $NO_3$ ). This leads to different implica-  
61 tions for the efficiency of SOA formation (Hallquist et al., 2009; Kiendler-Scharr et al., 2009; Mentel et  
62 al., 2009; O'Dowd et al., 2002). In most cases, SOA products are poorly characterized due to a scarcity  
63 of measurements (Martin et al., 2010).

64

65           Considering the overall size of the Amazon rainforest (5.4 million km<sup>2</sup> in 2001; Malhi et al.,  
66 2008) and the significant contribution of BVOC emissions from this vast forest to the global VOC  
67 budget (globally 1000 Tg of carbon yr<sup>-1</sup>; Guenther et al., 2012), measurements of total monoterpene  
68 emissions and mixing ratios from this ecosystem are scarce (Greenberg and Zimmerman, 1984; Helmig  
69 et al., 1998; Jardine et al., 2015, 2011, 2017; Karl et al., 2007; Rinne et al., 2002; Yáñez-Serrano et al.,  
70 2015). Speciated measurements are even more rare (Jardine et al., 2015, 2017; Kesselmeier et al., 2002;  
71 Kuhn et al., 2004). Yet, this information is essential for our understanding of the functioning of the Am-  
72 azon rainforest in atmospheric chemistry-climate interactions. Knowledge of these processes also serves  
73 to improve predictions of future changes in atmospheric composition and to assess the impact of  
74 changes in regional emissions and land use on global climate caused by Amazon deforestation.

75

76           In this study, we evaluate measurements of speciated rainforest monoterpene mixing ratios as a  
77 function of height in the canopy, season and diel cycle. This evaluation includes a comparison with a  
78 canopy exchange modelling system (MLC-CHEM, Multi-Layer Canopy Chemistry Exchange model) to  
79 support analysis of the measured temporal variability in speciated rainforest monoterpene mixing ratios  
80 inside the tropical rainforest canopy. The MLC-CHEM model was also selected since it has been al-  
81 ready extensively applied for site- to global-scale studies on atmosphere-biosphere exchange for tropi-  
82 cal rainforests (Ganzeveld et al., 2008, 2002; Ganzeveld and Lelieveld, 2004; Kuhn et al., 2010).

83

## 84 **2. Methodology**

85

### 2.1. Site

86           The site chosen for this study was the Amazon Tall Tower Observatory, ATTO (Andreae et al.,  
87 2015). This site is located in Central Amazonia (S 02° 08.647' W 58° 59.992'), 150 km NE of the clos-  
88 est large city, Manaus, Brazil. Due to the prevailing north-easterly wind direction, the influence of the  
89 Manaus plume is negligible and the measurements at this site can be considered to reflect pristine tropi-  
90 cal forest conditions affected by air masses that have passed over about 1000 km of undisturbed rainfor-  
91 est. The site is equipped with a 325 m tall tower as well as two smaller towers. This study was carried

92 out on the INSTANT tower, an 80-m walk-up tower located 600 m from the tall tower in easterly direc-  
93 tion. Sampling was performed on this tower below canopy top (mean canopy height 35 m) at two differ-  
94 ent heights (12 m and 24 m). For a comprehensive site description see Andreae et al. (2015).

## 95 96 2.2. Air sampling

97 Collection of ambient air samples on adsorbent tubes, for subsequent analysis by Gas Chroma-  
98 tography – Flame Ionization Detector (GC-FID), was made with two automated cartridge samplers de-  
99 scribed earlier (Kesselmeier et al., 2002; Kuhn et al., 2002, 2005) positioned at 12 and 24 m on the IN-  
100 STANT tower. The samplers consist of two main units, a cartridge magazine that holds the adsorbent-  
101 filled tubes and the control unit timing the process and recording the data. This latter unit also houses  
102 the pumps (Type N86KT, KNF Neuberger, Freiburg, Germany), pressure gauges, mass flow controllers  
103 and power supply. The cartridge magazine is equipped with solenoid valves controlling the inlet and  
104 outlet of up to 20 individual sampling adsorbent tubes. The system is a constant-flow device, with one  
105 cartridge position per loop used as a bypass for purging the system. Due to the compact weatherproof  
106 housings and the low power consumption, we were able to position one sampler at 24 m and the other  
107 one at 12 m, attached to the INSTANT tower booms with commercially available 50 mm aluminium  
108 clamps. The adsorbent tubes used for VOC sampling were filled with 130 mg of Carbograph 1 ( $90 \text{ m}^2$   
109  $\text{g}^{-1}$ ) followed by 130 mg of Carbograph 5 ( $560 \text{ m}^2 \text{ g}^{-1}$ ) sorbents. The size of the Carbograph particles  
110 was in the range of 20–40 mesh. Carbographs 1 and 5 were provided by L.A.R.A s.r.l. (Rome, Italy)  
111 (Kesselmeier et al., 2002). The samples were collected from 17 to 20 October 2015. Samples were  
112 taken for 30 min every hour at a flow of  $200 \text{ cm}^3 \text{ min}^{-1}$  (STP), leading to a collection of 6 L of air in  
113 each cartridge using the automatic sampler. Additional sampling was performed at 24 m with a GSA  
114 SG-10-2 personal sampler pump during the years 2012-2014. These earlier samples were collected in  
115 the same type of adsorbent tubes as for the automatic sampler, and were filled at  $167 \text{ cm}^3 \text{ min}^{-1}$  (STP)  
116 air flow for 20 min. These additional measurements took place on 19 and 28 November 2012; 1, 3 and 4  
117 March 2013; 11 to 14 June 2013; 22, 25 and 26 September 2013 and on 17 and 21 August 2014.

## 118 119 2.3. Instruments used for chemical analysis

### 120 2.3.1. Gas Chromatography –Flame Ionization Detector (GC-FID)

121 After collection, the adsorbent tubes were analysed at the Max Planck Institute for Chemistry  
122 (MPIC) using a Gas Chromatograph equipped with a Flame Ionization Detector (GC-FID, Model Auto-  
123 System XL, Perkin Elmer GmbH, Germany) for identification and quantification of the monoterpene  
124 species. Helium was used as carrier gas, and separation occurred on a 100 meter HP-1 column with 0.22  
125 mm inner diameter, coated with the non-polar dimethylpolysiloxane as stationary phase. The compound  
126 mixture collected in the adsorbent tubes was discharged into the gas stream with the help of a two-step  
127 desorption system (Model ATD400, Perkin Elmer, Germany). The samples were cryofocused in a cold  
128 trap at -30 °C filled with Carbograph 5, providing better defined peaks in the chromatograms. After-  
129 wards the cold trap was heated to 280°C and the pre-concentrated sample injected onto the column. The  
130 following temperature programme was used: (-10 to 40 °C at 20 °C min<sup>-1</sup>, 40 to 145 °C at 1.5 °C min<sup>-1</sup>,  
131 and 145 to 220 °C at 30 °C min<sup>-1</sup>). The separated compounds were quantified with a Flame Ionization  
132 Detector (FID). Identification was achieved through spiked injection of pure compounds. For a more  
133 detailed description see Kesselmeier et al., (2002).

134  
135 Calibration for VOCs containing no heteroatoms was achieved by using a standard gas mixture  
136 of isoprene and several n-alkanes (n-pentane, n-hexane, n-heptane, n-octane, n-nonane, and n-decane)  
137 (Apel-Riemer Environmental Inc., USA). In this case, it is assumed that the “effective carbon number”  
138 (Sternberg et al., 1962) is equal to the real carbon number of the molecules (Komenda, 2001), yielding a  
139 signal response that is proportional to the real carbon number. The monoterpenes identified and quanti-  
140 fied were  $\alpha$ -pinene, camphene, sabinene,  $\beta$ -pinene, myrcene,  $\alpha$ -phellandrene, 3-carene,  $\alpha$ -terpinene,  $p$ -  
141 cymene, limonene and  $\gamma$ -terpinene. Isoprene was also quantified. The detection limit for the GC-FID  
142 was 2 ppt (Bracho-Nunez et al., 2011).

### 2.3.2. Proton Transfer Reaction - Mass Spectrometer (PTR-MS)

Online total monoterpene mixing ratios were determined by a quadrupole Proton Transfer Reaction - Mass Spectrometer, PTR-MS (Ionicon Analytic, Austria). The PTR-MS was operated under standard conditions (2.2 mbar drift pressure, 600 V drift voltage, with an E/N of 142 Townsend (Td)). In addition to weekly humidity dependent calibrations, hourly background measurements were performed with a catalytic converter (Supelco, Inc. with platinum pellets heated to >400°C). A gravimetrically prepared multicomponent standard for calibration was obtained from Apel & Riemer Environmental, USA. The measurements were carried out at two different heights (12 and 24 m) with the PTR-MS switching sequentially between each height at 2 min intervals. The inlet lines were made of PTFE (9.5 mm OD), insulated and heated to 50 °C, and had PTFE particle inlet filters at the intake end. The compounds of interest for this study were isoprene ( $m/z$  69) and the sum of monoterpenes ( $m/z$  137). The limit of detection (LOD) of the PTR-MS for total monoterpenes was 0.1 ppb and 0.2 ppb for isoprene, determined as  $3\sigma$  of the background noise. More information about the gradient system and PTR-MS operation at ATTO can be found elsewhere (Nölscher et al., 2016; Yáñez-Serrano et al., 2015).

### 2.4. Multi-Layer Canopy Chemistry Exchange model (MLC-CHEM)

To analyse the magnitude and temporal variability of the observed monoterpene concentrations inside and above the forest canopy, we applied the Multi-Layer Canopy Chemistry Exchange Model (MLC-CHEM), driven by the observed micro-meteorology and ozone surface layer mixing ratios. MLC-CHEM was originally developed and implemented in a single-column model (SCM). It is set up also in a global chemistry and climate-modelling system to assess the role of canopy processes in local-to global-scale atmosphere-biosphere exchange of nitrogen oxides (Ganzeveld et al., 2008, 2002; Kuhn et al., 2010). The model's generalized representation of chemistry, dry deposition, emissions and turbulent mixing allows studying the role of canopy interactions in determining atmosphere-biosphere exchange fluxes and in-canopy and surface layer mixing ratios of, e.g., ozone ( $O_3$ ), nitrogen oxides ( $NO_x$ ) and biogenic volatile organic compounds (BVOCs). The BVOC emissions are calculated according to MEGAN (Guenther et al., 2006), considering the vertical distribution of biomass and direct as well as

171 diffuse radiation to calculate leaf-scale BVOC emissions. The current implementation of canopy chem-  
172 istry in MLC-CHEM considers, in addition to standard photo-chemistry involving O<sub>3</sub>, NO<sub>x</sub>, methane  
173 (CH<sub>4</sub>) and carbon monoxide (CO), the role of non-methane hydrocarbons including isoprene, and a se-  
174 lection of hydrocarbon oxidation products such as formaldehyde, higher aldehydes and acetone. Oxida-  
175 tion of the monoterpenes by OH, O<sub>3</sub> and NO<sub>3</sub> is taken into account, but the role of the monoterpene oxi-  
176 dation products in photo-chemistry is not considered in the current implementation of the chemistry  
177 scheme in MLC-CHEM. For this study, we have extended MLC-CHEM to consider, besides the already  
178 included compounds α-pinene and β-pinene, the observed monoterpene species, α-terpinene, limonene  
179 and myrcene. The monoterpene basal leaf-scale monoterpene emission factors have been selected such  
180 that the model simulates monoterpene mixing ratios of comparable magnitude compared to the cam-  
181 paign-average observed mixing ratios. In the evaluation of simulated and observed mixing ratios we  
182 mainly focus on comparison of the simulated and observed temporal variability being determined by the  
183 differences in canopy processes for contrasting nocturnal and daytime conditions. For the model simula-  
184 tion, the basal emission factors were 0.18 μg C g<sup>-1</sup> h<sup>-1</sup> for α-pinene, 0.04 μg C g<sup>-1</sup> h<sup>-1</sup> for β-pinene, 0.11  
185 μg C g<sup>-1</sup> h<sup>-1</sup> for α-terpinene, 0.9 μg C g<sup>-1</sup> h<sup>-1</sup> for limonene and 0.18 μg C g<sup>-1</sup> h<sup>-1</sup> for myrcene. Note the  
186 selected relative high basal emission flux for limonene is required to arrive at simulated mixing ratios  
187 comparable to the observed ones. Regarding the physical sinks; dry deposition of gases including the  
188 BVOC compounds depends on their uptake resistances calculated according to Wesely's (1989) parame-  
189 terization, which estimates these uptake resistances based on the compounds' solubility and reactivity.

190

191 The simulations with MLC-CHEM were constrained with the observed surface layer net radia-  
192 tion (above the canopy only), wind speed, relative humidity and O<sub>3</sub> mixing ratios as well as the temper-  
193 atures measured above and inside the canopy (8 different heights including 12 and 24m) from 17 to 20  
194 October 2015, coinciding with the measurement dates. These simulations represent a set-up of MLC-  
195 CHEM distinguishing six canopy levels with a canopy height of 30 m, implying canopy layers with a  
196 thickness of 5 m. Furthermore, we assumed a Leaf Area Index (LAI) of 5 m<sup>2</sup> m<sup>-2</sup> and a Leaf Area Den-

197 sity (LAD) profile such that about 70% of this biomass is present in the top 15 m of the canopy, as pre-  
198 viously observed at other tropical rainforest sites (Nölscher et al., 2016). Monoterpene emissions by  
199 vegetation were simulated using a temperature-only dependent emission flux as a function of the  
200 amount of biomass in each layer and the measured canopy temperature profiles interpolating between  
201 the 0.4 m and 26 m temperature sensors. Meteorological observations for 18 October were missing and  
202 therefore MLC-CHEM was constrained for this day by first-order estimates of the diurnal cycles in radi-  
203 ation, air and surface temperatures, relative humidity and wind speed comparable to the previous and  
204 subsequent day's meteorological conditions.

205

### 206 **3. Results and discussion**

#### 207 3.1. Time series and diel cycles

208 The continuous online PTR-MS measurements were compared with off-line GC-FID samples  
209 over the course of 3 days in October 2015 (Figure 1). The close agreement between the two measure-  
210 ment techniques provides confidence that almost all monoterpenes present in ambient air at the site  
211 were being measured. Note that in this comparison, *p*-cymene (an aromatic monoterpene) was removed  
212 from the calculations as the PTR-MS does not detect it on  $m/z$  137. The observed differences in the  
213 monoterpene chemodiversity in the rainforest canopy atmosphere were regarded to be driven by differ-  
214 ences in emission, reactivity with the oxidizing species, physical removal processes and turbulent mix-  
215 ing conditions.

216

217 The total monoterpene mixing ratios were higher during the day, when temperature and solar  
218 radiation were at their maxima. Most of the observed distinct diurnal cycle in total monoterpene mixing  
219 ratios could be attributed to  $\alpha$ -pinene, which was the dominant species during daytime (0900h to 1700h)  
220 with mixing ratios as large as (average  $\pm$  standard deviation)  $0.33 \pm 0.04$  and  $0.38 \pm 0.21$  ppb at 12 and 24  
221 m respectively, and  $0.15 \pm 0.05$  and  $0.11 \pm 0.06$  ppb for the night (2000h to 0500h) at 12 and 24 m. The  
222 second most abundant monoterpene species was limonene, with observed average daytime mixing ratios

223 of  $0.18\pm 0.09$  and  $0.19\pm 0.12$  ppb at 12 and 24 m, respectively, and  $0.18\pm 0.01$  and  $0.14\pm 0.07$  ppb for the  
224 night time at 12 and 24 m.

225  
226 When comparing our results to previously published studies, we observed consistent differences  
227 with other regions of the Amazon rainforest. For instance, Kesselmeier et al. (2002) studied the seasonal  
228 monoterpene speciation in the Rondonia rainforest in southern Amazonia. Even though they found the  
229 same monoterpene species as presented in this study, their individual abundances were very different  
230 compared to the mixing ratios for the dry season at the ATTO site.  $\alpha$ -pinene and limonene were much  
231 higher at ATTO than in Rondonia, whereas camphene was substantially lower. In the case of  $\beta$ -pinene,  
232 the abundance measured at ATTO was much lower than at other Amazonian sites (Andreae et al., 2002;  
233 Karl et al., 2007). Given that emission patterns are highly dependent on species, environmental condi-  
234 tions and stresses, these differences underline that it cannot be assumed that the same speciation and  
235 emission rates of monoterpenes exist throughout the vast Amazon basin.

236  
237 Furthermore, the difference between the 12 and 24 m height total monoterpene mixing ratios  
238 was minor given the variance of the measurements, but there was a tendency for the difference to be  
239 more pronounced during night time (Table 1). These more pronounced differences between the meas-  
240 urement heights could be also due to an enhanced sensitivity of nocturnal mixing ratios to small  
241 changes in source and sink terms for the suppressed mixing conditions prevailing during the night time.

242  
243 The continuous online measurements by the quadrupole PTR-MS indicated a clear diurnal cycle  
244 in the measured mixing ratios of the sum of monoterpenes, which has been reported previously from  
245 this site (Yáñez-Serrano et al., 2015). In order to assess the effect of each individual monoterpene spe-  
246 cies, we further investigated their diurnal cycles as obtained by the off-line GC-FID samples. The meas-  
247 ured diel cycles for the most relevant monoterpene species at the ATTO site were very similar at both  
248 heights. We also compared the measured diel cycle of isoprene as measured by the GC-FID with the ob-  
249 served diel cycle for the different monoterpene species for 12 and 24 m. The compounds that showed a

250 diurnal cycle similar to isoprene were  $\alpha$ -pinene and  $p$ -cymene (Figure 2). This could be due to the emis-  
251 sion of  $\alpha$ -pinene and  $p$ -cymene being dependent on light and temperature, analogous to isoprene. How-  
252 ever, during the night both monoterpenes were also present, albeit at lower mixing ratios, and the noc-  
253 turnal mixing ratios of the monoterpenes did not decrease as much as isoprene. This has also been noted  
254 in previous studies (Yáñez-Serrano et al., 2015).

255  
256 Despite the higher mixing ratios of limonene compared to other monoterpene species (other than  
257  $\alpha$ -pinene), it was not possible to distinguish any clear diel pattern in the average data for this species  
258 (see Figure 2).  $\beta$ -Pinene and  $\alpha$ -terpinene likewise showed no obvious diel pattern in the rainforest air,  
259 but were found to be above the detection limit of the GC-FID of 2 ppt.

260  
261 In contrast to plant species of cooler climates, such as spruce, which emit terpenes from pools  
262 (Ghirardo et al., 2010; Lerdau et al., 1997), Amazonian plant species have been found to show an emis-  
263 sion dependency on light and temperature (Bracho-Nunez et al., 2013; Jardine et al., 2015; Kuhn et al.,  
264 2002, 2004). This could partly explain the diurnal pattern of  $\alpha$ -Pinene mixing ratios, which exhibit some  
265 relation to a light and temperature dependent emission flux (Kuhn et al., 2002; Rinne et al., 2002;  
266 Williams et al., 2007). However, this behaviour was not observed for all monoterpene species. There-  
267 fore, the observed diurnal cycles of some monoterpene species might be related to a stronger tempera-  
268 ture response.

### 269 270 3.2. Chemodiversity

271 The chemical speciation (or chemodiversity) of monoterpenes relates to the relative abundances  
272 of the different monoterpene species in the sampled air.  $\alpha$ -Pinene, limonene, myrcene,  $p$ -cymene and  $\beta$ -  
273 pinene represented more than 85% of the total monoterpene mixing ratio (Figure 3). During the day  
274 (0900h to 1700h)  $\alpha$ -pinene had an average abundance (average $\pm$ standard deviation) of  $46\pm 25\%$  and  
275  $36\pm 4\%$  of the total monoterpene mixing ratios at 24 and 12 m, respectively, and was the dominant mon-  
276 oterpene in this study overall. However, during the night (2000h to 0500h), its relative abundance  
277 dropped to  $25\pm 13\%$  and  $25\pm 9\%$  at 24 and 12 m, respectively. In contrast, limonene made up  $23\pm 15\%$

278 and  $20\pm 10\%$  of the monoterpenes at 24 and 12 m, respectively, by day, and increased during night time  
279 to  $33\pm 15\%$  and  $26\pm 16\%$  at 24 and 12 m. Thus, there was a tendency towards some differences in mono-  
280 terpene species abundances between day and night. These were mainly due to the nocturnal decreases in  
281  $\alpha$ -pinene and the nocturnal relative increase in limonene. It is plausible that the observed decrease in  $\alpha$ -  
282 pinene mixing ratios could be due to decreased vegetation emission, as reduced chemical destruction  
283 due to very low OH concentrations at night would lead to an increase in the nocturnal  $\alpha$ -pinene mixing  
284 ratios.

285

286 Even though there were clear differences between the absolute and relative abundances of some  
287 monoterpene species during day and night, there were no clear changes in the vertical gradients (e.g. for  
288  $\alpha$ -pinene night time averages were  $0.15\pm 0.05$  ppb for 12 m and  $0.11\pm 0.06$  ppb at 24 m). For the day, the  
289 apparent difference in the abundance of  $\alpha$ -pinene was due to a single outlier data point covering 30  
290 minutes at noon on 19 October 2015 at 24 m, when the  $\alpha$ -pinene mixing ratio doubled. This increase  
291 could not be explained, although it could be related to a strong change in wind speed an hour before the  
292 measurement, when the wind was blowing from the North. In general, our observations indicate that the  
293 abundance of monoterpene species does not vary much over the heights selected (12 and 24 m) within  
294 the canopy. This is consistent with the results by Kesselmeier et al. (2000), where the monoterpene  
295 composition at the rain forest floor was comparable to the above-canopy composition at their site.

296

### 297 3.3. Reactivity

298 The variability of the oxidants (OH, O<sub>3</sub> and NO<sub>3</sub>) present in the Amazon air is important when  
299 considering the impact that monoterpenes can have on the oxidative regime in the Amazon region and  
300 Brazil in general. Hydroxyl radicals are produced mainly during the day via ozone photolysis. Low lev-  
301 els of OH can be also generated by the reaction of ozone with doubly bonded species (e.g. monoter-  
302 penes and sesquiterpenes) even at night. In this assessment, we considered the monoterpene contribu-  
303 tions to OH reactivity by day only. In contrast, NO<sub>3</sub> is photolytically destroyed during the day, but can  
304 become significant at night, so we assessed the impact of monoterpenes on NO<sub>3</sub> reactivity at night.

305 Even though in the Amazon rainforest ozone levels are low (~10-20 ppb) compared to other areas of the  
306 world (e.g., Williams et al., 2016), it is nevertheless present, and some monoterpenes are extremely re-  
307 active towards ozone. Table 2 gives an overview of the lifetime and reactivity (which is defined as reac-  
308 tion rate constant (oxidant i.e. OH)\*[monoterpene species]) to 1 ppb of all the investigated monoterpene  
309 species for these three oxidants. For calculating the lifetime of the different monoterpenes as presented  
310 in Table 2, typical oxidant concentrations for the Amazon rainforest conditions were used. For OH a  
311 mean value of  $7 \times 10^5$  molecules  $\text{cm}^{-3}$  was used as representative of the site (Spivakovsky et al., 2000).  
312 For ozone reactivity calculations, 12 ppb was used, as this mixing ratio was observed during the meas-  
313 urement period.  $\text{NO}_3$  mixing ratios were taken from the MLC-CHEM model simulations that predicted  
314 mixing ratios of ~0.4 ppt.

315

316 While  $\alpha$ -pinene, limonene and myrcene were the most abundant species, their relative contribu-  
317 tion to total monoterpene reactivity was not proportional to their abundances. The most abundant mono-  
318 terpene,  $\alpha$ -pinene was not the dominant sink for the oxidants. In particular,  $\alpha$ -terpinene dominated  
319 ozone reactivity associated with monoterpene abundance both during the day and night, as well as the  
320 nocturnal nitrate reactivity, despite the low mixing ratios measured for this compound (Table 2).

321

322 The monoterpene ozone reactivity was comparable between day ( $1.37 \times 10^{-6} \text{ s}^{-1}$ ) and night ( $1.12 \times 10^{-6} \text{ s}^{-1}$ ).  
323  $\alpha$ -Terpinene dominated the monoterpene-ozone chemistry, followed by myrcene and limonene. Despite  
324 the relatively high abundance of  $\alpha$ -pinene ( $46 \pm 25\%$ ; average mixing ratio and standard deviation during  
325 the day was  $0.34 \pm 0.04$  ppb at 12 m), its contribution to ozone reactivity with respect to other monoter-  
326 pene species was only  $11 \pm 7\%$  and  $3 \pm 1\%$  at 24m, during the day and night, respectively, and  $2 \pm 1\%$  for  
327 both day and night at 12 m (Figure 4). As previously noted, the differences in ozone reactivity between  
328 heights were negligible for the night and slightly higher at 24 m during the day. As ozone mixing ratios  
329 are quite similar for both heights during day and night (11.4 ppb at 12 m and 10.4 ppb at 24 m during  
330 night, and 16.1 ppb at 12 m and 15.6 at 24 m during the day), the higher abundance of  $\alpha$ -pinene during  
331 the day, and the lower  $\alpha$ -terpinene mixing ratios at 24 m during the day mainly explain these changes in

332 monoterpene-ozone reactivity. It is important to note that these results are derived from a relative abun-  
333 dance analysis, and unmeasured monoterpene species could change the proportions, although given the  
334 close similitude between PTR-MS and GC-FID measurements shown in Figure 1 this is unlikely. On  
335 the other hand, very reactive species which could dominate reactivity, may be present in very low con-  
336 centrations, which our measurements capabilities would not allow being detected.

337

338 The monoterpene reactivity towards the  $\text{NO}_3$  radical during the night was also dominated by  $\alpha$ -  
339 terpinene ( $40\pm 36\%$  and  $42\pm 27\%$ , for 24 and 12 m, respectively), although contributions of limonene  
340 ( $30\pm 13\%$  and  $25\pm 14\%$ , for 24 and 12 m, respectively),  $\alpha$ -pinene ( $11\pm 6$  and  $11\pm 4\%$ , for 24 and 12 m,  
341 respectively), and myrcene ( $13\pm 11$  and  $16\pm 12\%$ , for 24 and 12 m, respectively) were also significant.  
342 No significant differences between the reactivities at different heights were observed, suggesting a rather  
343 homogeneous chemical regime regarding monoterpene chemical destruction within the canopy (from 12  
344 to 24 m). However, note that this finding reflects the use of a single simulated  $\text{NO}_3$  mixing ratio due to  
345 the absence of direct measurements in the Amazon rainforest, which prevents us from drawing any fur-  
346 ther conclusion. Our OH reactivity estimates demonstrate the important role of myrcene with its higher  
347 reactivity towards OH due to its acyclic nature, especially at 12 m, where myrcene was more abundant.  
348 The total OH reactivity for the sum of monoterpenes was calculated to be  $2.4$  and  $3.4 \text{ s}^{-1}$  for 24 and 12  
349 m, respectively.

350

351 As demonstrated in this data set, chemically speciated measurements are very important for un-  
352 derstanding how monoterpenes affect Amazon air chemistry dependent on time of day and season, as  
353 each monoterpene species has a different reactivity. Therefore, a lower abundance of a certain monoter-  
354 pene species could not necessarily be related to a lower vegetation emission, but also to a higher reac-  
355 tivity with atmospheric oxidants. Despite the small amount of  $\alpha$ -terpinene present in the atmosphere, it  
356 can profoundly affect reactivity due to its fast reaction rate (its lifetime, according to the oxidant mixing  
357 ratios stated above, can be 103, 2 and 11 minutes to OH,  $\text{O}_3$  and  $\text{NO}_3$ , respectively, Neeb et al., 1997).  
358 In terms of total OH reactivity accounted for by the monoterpenes, the values of this study are very low

359 compared to the total OH reactivity measurements by Nölscher et al. (2016), with a mean of total OH  
360 reactivity for the dry season of  $32 \text{ s}^{-1}$ , mostly dominated by isoprene chemistry. This suggests that the  
361 monoterpenes contributed only a small fraction to the total OH reactivity at the ATTO site during the  
362 investigated time period. This study demonstrates that the abundance does not relate to the importance  
363 in chemical reactivity, and species that are usually not considered by atmospheric chemistry models due  
364 to their modest mixing ratios might actually play a dominant role in the monoterpene atmospheric  
365 chemistry. Therefore, it is questionable to generalize the representation of terpene chemistry in models  
366 (Hallquist et al., 2009) using one or two monoterpene species only.

367

368 The gas-phase oxidation of the monoterpenes in the Amazon has numerous impacts on the envi-  
369 ronment, including the production of a multitude of new compounds that are generally longer lived than  
370 the primary emissions, increasing the lifetimes and particle production potential of certain compounds  
371 by suppressing oxidant availability. Moreover, production of OH due to the ozonolysis of monoterpenes  
372 is known to occur (Paulson et al., 1999). The production strength varies depending on the position of  
373 the double bonds, if there is more than one (Herrmann et al., 2010). Furthermore, the products of the  
374 reaction can be manifold. For instance, when  $\alpha$ -pinene is oxidized by OH, especially at low nitrogen ox-  
375 ides mixing ratios, pinonaldehyde is formed in high yields (Eddingsaas et al., 2012). Chemical pro-  
376 cessing of  $\alpha$ -pinene can also result in a further production of different monoterpenes such as the reaction  
377 of  $\alpha$ -pinene with nitrate during the night, which can lead to the formation of  $\rho$ -cymene (Gratien et al.,  
378 2011).

379

380 The implications of the measured monoterpene abundances for SOA formation at the ATTO site  
381 are difficult to quantify, because the SOA formation yield is dependent on many factors. For example, it  
382 depends on the pre-existing organic aerosol mass into which these products can be absorbed (Griffin et  
383 al., 1999), and thus the SOA yield can vary between regions with similar monoterpene mixing ratios  
384 and different aerosol mass loadings. It also varies strongly between different oxidants and terpene spe-  
385 cies. For instance,  $\alpha$ -pinene forms negligible aerosol mass under  $\text{NO}_3$  oxidation (Fry et al., 2014),  
386 whereas there is production of organic aerosols when the oxidation of  $\alpha$ -pinene involves  $\text{O}_3$  (Ehn et al.,

2014) and OH (Eddingsaas et al., 2012). Monoterpenes containing endocyclic double bonds (e.g.  $\alpha$ -pinene, 3-Carene) or open chains (e.g. myrcene) tend to form less aerosols mass from ozonolysis than monoterpenes with exocyclic double bonds (e.g.  $\beta$ -pinene, sabinene, Hatakeyama et al., 1989; Hoffmann et al., 1997). Following the equation established by Bonn et al. (2014, Eq. 5 in text), we were able to estimate the potential aerosol particle number formation rate initiated by monoterpene species only ( $1 \times 10^{-5}$  to  $5 \times 10^{-5}$   $\text{cm}^{-3} \text{s}^{-1}$  at 24 m) assuming steady state conditions for radicals. Those were found to be approximately two orders of magnitudes smaller than the calculated potential new aerosol particle formation rate caused by oxidation products of sesquiterpenes. Our calculations assume mixing ratios of sesquiterpenes of 0.2 ppb revealing potential formation rates of ( $1 \times 10^{-3}$  and  $4.5 \times 10^{-3}$   $\text{cm}^{-3} \text{s}^{-1}$  at 24 m) based on previous measurements in the Amazon (Jardine et al., 2011), which are remarkably smaller than observed at mid-latitude conditions (Bonn et al., 2014). Furthermore, the level of NO present (nitric oxide) also affects the potential aerosol growth (Wildt et al., 2014) and yield (Sarrafzadeh et al., 2016) at low BVOC/NO<sub>x</sub> ratios). As the theory assumes contributions of larger organic peroxy radicals (RO<sub>2</sub>), which are destroyed by reactions, e.g. with NO, increasing NO<sub>x</sub> at constant BVOC mixing ratio will decrease the BVOC/NO<sub>x</sub> ratio and lead to a decline in SOA yield. Our calculations showed this effect, with a change of NO from 0.2 ppb to 1 ppb leading to a decrease in the formation rate at a diameter of 3 nm. This interdependence calls for a consistent consideration of the BVOC and NO<sub>x</sub> exchange in aerosol formation and growth studies.

### 3.4. Seasonality

By examining GC-FID data collected in previous campaigns, an intra- and inter-annual comparison can be made. Total monoterpene averages for each season were calculated from 1100h to 1600h at 24 m. Based on these data, we distinguished the monoterpene mixing ratios representative for the dry season, the wet season and the wet-to-dry transition. The dry season conditions were represented by measurements collected in November 2012, September 2013, August 2014, and the measurements from this study in October 2015. The wet season measurements were collected in March 2013 and the wet-to-dry transition measurements were collected in June 2013. For the dry season conditions, the total mono-

414 terpene mixing ratios were substantially higher (1.02 ppb) compared to the observed monoterpene mix-  
415 ing ratios in the wet season (0.14 ppb) and the wet-to-dry transition season (0.18 ppb) (Figure 5). This  
416 coincides with the occurrence of the highest radiation levels and temperatures as well as the lowest pre-  
417 cipitation during these dry season measurement campaigns. During the wet season, the total monoter-  
418 pene mixing ratios were lowest, while during the transition season in June, they were slightly higher.

419  
420 For each season, an average monoterpene chemodiversity distribution is shown in Fig. 5. During  
421 the dry seasons, the chemodiversity seems relatively similar ( $39.4\pm 4\%$  for  $\alpha$ -pinene,  $20.3\pm 3\%$  for limo-  
422 nene), whereas it slightly changes during the wet season, and dramatically changes during the wet-to-  
423 dry transition. The reason for this difference in June could be related to changes in the phenology, as  
424 demonstrated at a Central Amazonian site (Alves et al., 2016; Lopes et al., 2016). Furthermore, during  
425 the dry season of 2015 a very strong El Niño event took place, leading to extremely dry conditions ob-  
426 served region-wide (Jardine et al., 2017).

427  
428 It has been shown previously that the amounts and speciation of monoterpenes vary strongly ac-  
429 cording to plant species and leaf developmental stage. For instance, Bracho-Nunez et al. (2011) found  
430 young leaves of the some Mediterranean plant species to emit more  $\alpha$ -pinene and mature leaves to emit  
431 *e*-ocimene, *z*-ocimene and myrcene, but not  $\alpha$ -pinene. Some species have been found to be higher emit-  
432 ters of  $\alpha$ -pinene (i.e. *Hevea spruceana*), whereas others are higher emitters of myrcene (i.e. *Quercus*  
433 *coccifera*, Bracho-Nunez et al., 2013). The leaf developmental stage is also important, as reported for  
434 flushing young leaves emitting monoterpenes, in contrast to the isoprene emission of mature leaves of  
435 the same plant species (Kuhn et al., 2004). Such a behaviour could explain the lower mixing ratios and  
436 different chemodiversity found in June. During this time of the year, leaf flushing takes place in the  
437 Central Amazon region (Alves et al., 2016; Lopes et al., 2016). Under these conditions, lower  $\alpha$ -pinene  
438 mixing ratios were found as compared to the dry season, when young leaves reach mature levels. There-  
439 fore, the seasonality in Amazon forest monoterpene emissions might depend more on the changes in ag-  
440 gregated canopy phenology than on the seasonality of climate drivers (Wu et al., 2016). Our study

441 shows that chemodiversity remains relatively constant during at least the dry seasons, but changed be-  
442 tween different seasons. Therefore, the implications to the atmosphere are different for each monoter-  
443 pene species. Kesselmeier et al. (2002) also showed this type of behaviour in their study, where they did  
444 not find a strong difference in total mixing ratios, but different chemodiversity between seasons, likely  
445 expressing differences in seasonal plant developments and atmospheric reactivities, which should be  
446 accounted for in model implementations at the ATTO site.

### 447 448 3.5. Modelling analysis

449 To further support our analysis of the observed magnitude as well as temporal variability in the  
450 monoterpene mixing ratios inside the forest canopy, we used MLC-CHEM to: 1) explore how well the  
451 model represents the measured mixing ratios and 2) to assess the role of the different in-canopy pro-  
452 cesses in explaining the diel cycle of the observed monoterpene mixing ratios at the ATTO site.

453  
454 From Fig. 6, which shows a comparison of the simulated (12.5 and 22.5 m) and observed (12  
455 and 24 m) speciated monoterpene mixing ratios from 17 to 20 October 2015, it can be inferred that the  
456 simulated speciated monoterpene mixing ratios are of comparable magnitude to the measured observa-  
457 tions. This comparison regarding the magnitude of observed and simulated mixing ratios serves mainly  
458 to assess the validity of the required selection of basal emission fluxes for the different monoterpene  
459 compounds. A more relevant result seems to be the overall quite good agreement between the simulated  
460 and observed temporal variability in monoterpene mixing ratios. Note that we also conducted a simula-  
461 tion in which we applied temperature and light dependent monoterpene emission flux. However, those  
462 simulations did not follow the observed magnitudes and temporal variability as well as the model simu-  
463 lations considering monoterpene emissions that only depend on temperature.

464  
465 The generally quite good agreement between the simulated and observed monoterpene mixing  
466 ratios, except of an overestimation of simulated  $\alpha$ -pinene mixing ratios for 17 October, expresses the

467 overall result of temporally varying emissions, in-canopy chemistry, turbulent mixing and deposition.  
468 The latter also involves a potentially important role of deposition to wet leaf surfaces (the inferred wet  
469 surface uptake resistances for the monoterpenes are  $\sim 300 \text{ s m}^{-1}$ , similar to values reported by Zhou et  
470 al., (2017), MLC-CHEM uses relative humidity as a proxy for the fraction of the leaf surface being wet,  
471 Lammel, 1999; Sun et al., 2016). This results in substantially smaller estimates of canopy wetness on 17  
472 October compared to the following days, which partly explains the simulated high  $\alpha$ -pinene mixing ra-  
473 tios. The simulated  $\alpha$ -pinene mixing ratios for 18-20 October, with inferred wet surface fractions up to 1  
474 during the night and  $\sim 0.5$  during daytime, are in much better agreement with the observations. Regard-  
475 ing the comparison of the simulated observed mixing ratios for some of the other monoterpenes, the  
476 simulated  $\beta$ -pinene, limonene, and myrcene mixing ratios, especially at 12.5 m seem to capture the ob-  
477 served temporal variability quite well. Note that this result for limonene reflects the use of a high leaf  
478 basal emission factor ( $0.9 \mu\text{g C g}^{-1} \text{ hr}^{-1}$ ) required to simulate mixing ratios reaching up to 0.4 ppb. These  
479 MLC-CHEM simulations were also used to infer how much of the actual emission flux escapes the can-  
480 opy, expressed by the calculated atmosphere-biosphere limonene flux divided by the canopy emission  
481 flux of limonene. This ratio reaches a maximum value of 0.5 around noontime, implying that these  
482 model simulations indicate that at the middle of the day, about 50% of the emitted limonene is removed  
483 inside the canopy by in-canopy oxidation and deposition. During night time, this ratio reaches a mini-  
484 mum  $< 0.1$  indicating simulation of very efficient in-canopy removal.

485

486 These modelling results should be interpreted with caution, also given that some of the simu-  
487 lated processes cannot be evaluated due to missing observations of canopy wetness as well as the uptake  
488 efficiency of monoterpenes by wet surfaces. It should be considered that the simulated removal of mon-  
489oterpenes by wet canopy surfaces could also compensate for a misrepresentation of other canopy pro-  
490cesses, e.g., reduced emissions from wet canopy surfaces or an underestimation of the oxidation effi-  
491ciency. Further analysis of the model simulated process tendencies (Ganzeveld et al., 2008) indicates  
492only small changes in the simulated source of the monoterpenes over the 4-day period. Regarding the  
493sink of, for example,  $\alpha$ -pinene, chemical destruction of  $\alpha$ -pinene oxidation by  $\text{O}_3$ ,  $\text{OH}$  and  $\text{NO}_3$  appears

494 to be a relative small term, with the overall sink being dominated by deposition to wet surfaces showing  
495 quite large temporal variability. Consequently, the quite reasonable agreement between simulated and  
496 observed temporal variability in monoterpene mixing ratios indicates that deposition to wet surfaces  
497 may play an important role in monoterpene atmosphere-biosphere exchange. This should be further cor-  
498 roborated, calling for experiments to determine the actual efficiency (and mechanisms) of uptake of  
499 monoterpenes by wet canopy surfaces.

#### 500 4. Conclusions

501 This study presents an analysis of the measured monoterpene chemodiversity at the Amazon  
502 tropical forest measurement site, ATTO. The results showed a distinctly different chemical speciation  
503 between day and night, whereas there were little vertical differences in speciation within the canopy (12  
504 and 24 m). Furthermore, inter- and intra-annual results demonstrate similar chemodiversity during the  
505 dry seasons analysed, but a change of chemodiversity with season, similar to the seasonal measurements  
506 performed by Kesselmeier et al. (2002). Furthermore, reactivity calculations demonstrated that higher  
507 abundance of a monoterpene species does not automatically imply higher reactivity, as the most abun-  
508 dant compounds may not be the most atmospheric chemically relevant compounds, or the relative con-  
509 tribution of different monoterpenes may change with time. Our calculations support the view that the  
510 role of canopy exchange may be erroneously estimated when not taking into account speciation-based  
511 reactivity in models. Moreover, simulations with a canopy exchange modelling system to assess the role  
512 of canopy interactions compared relatively well with the observed temporal variability in speciated  
513 monoterpenes, but also indicate the necessity of more experiments to enhance our understanding of in-  
514 canopy sinks of these compounds.

515

#### 516 5. Data Availability

517 Even though the data are still not available in any public repository, the data are available upon  
518 request from the main author.

519

#### 520 6. Acknowledgements

The authors thank the Max Planck Society and the Instituto Nacional de Pesquisas da Amazonia for continuous support. Furthermore, we acknowledge the support by the ATTO project (German Federal Ministry of Education and Research, BMBF funds 01LB1001A; Brazilian Ministério da Ciência, Tecnologia e Inovação FINEP/MCTI contract 01.11.01248.00), UEA and FAPEAM, LBA/INPA, and SDS/CEUC/RDS-Uatumã. In particular, EB acknowledges the support of BmBf project ATTO (01LK1602B). We would especially like to thank all the people involved in the logistical support of the ATTO project, in particular Reiner Ditz and Hermes Braga Xavier. We acknowledge the micrometeorological group of INPA/LBA for their collaboration concerning the meteorological parameters, with special thanks to Antonio Huxley and Leonardo Oliveira. We also want to thank Matthias Sörgel, Anywhere Tsokankunku and Rodrigo de Souza for help with the ozone measurements. We are grateful to Nina Knothe for logistical help. We greatly acknowledge Guenther Schebeske for the GC-FID analysis. We would also like to thank Thomas Klüpfel, Tomas Chor and Emilio Hoeltgebaum for their help during sampling. This paper contains results of research conducted under the Technical/Scientific Cooperation Agreement between the National Institute for Amazonian Research, the State University of Amazonas, and the Max-Planck-Gesellschaft e.V.; the opinions expressed are the entire responsibility of the authors and not of the participating institutions.

## 7. References

- Alves, E. G., Jardine, K., Tota, J., Jardine, A., Yáñez-Serrano, A. M., Karl, T., Tavares, J., Nelson, B., Gu, D., Stavrou, T., Martin, S., Artaxo, P., Manzi, A. and Guenther, A.: Seasonality of isoprenoid emissions from a primary rainforest in central Amazonia, *Atmos. Chem. Phys.*, 16(6), 3903–3925, doi:10.5194/acp-16-3903-2016, 2016.
- Andreae, M. O., Artaxo, P., Brandao, C., Carswell, F. E., Ciccioli, P., da Costa, A. L., Culf, A. D., Esteves, J. L., Gash, J. H. C., Grace, J., Kabat, P., Lelieveld, J., Malhi, Y., Manzi, A. O., Meixner, F. X., Nobre, A. D., Nobre, C., Ruvivo, M., Silva-Dias, M. A., Stefani, P., Valentini, R., von Jouanne, J. and Waterloo, M. J.: Biogeochemical cycling of carbon, water, energy, trace gases, and aerosols in Amazonia: The LBA-EUSTACH experiments, *J. Geophys. Res.*, 107(D20), 8066, doi:8066 10.1029/2001jd000524, 2002.
- Andreae, M. O., Acevedo, O. C., Araújo, A., Artaxo, P., Barbosa, C. G. G., Barbosa, H. M. J., Brito, J., Carbone, S., Chi, X., Cintra, B. B. L., da Silva, N. F., Dias, N. L., Dias-Júnior, C. Q., Ditas, F., Ditz, R., Godoi, A. F. L., Godoi, R. H. M., Heimann, M., Hoffmann, T., Kesselmeier, J., Könemann, T., Krüger, M. L., Lavric, J. V., Manzi, A. O., Lopes, A. P., Martins, D. L., Mikhailov, E. F., Moran-Zuloaga, D., Nelson, B. W., Nölscher, A. C., Santos Nogueira, D., Piedade, M. T. F., Pöhlker, C., Pöschl, U., Quesada, C. A., Rizzo, L. V., Ro, C.-U., Ruckteschler, N., Sá, L. D. A., de Oliveira Sá, M., Sales, C. B., dos Santos, R. M. N., Saturno, J., Schöngart, J., Sörgel, M., de Souza, C. M., de Souza, R. A. F., Su, H., Targhetta, N., Tóta, J., Trebs, I., Trumbore, S., van Eijck, A., Walter, D., Wang, Z., Weber, B., Williams, J., Winderlich, J., Wittmann, F., Wolff, S. and Yáñez-Serrano, A. M.: The Amazon Tall Tower Observatory (ATTO): overview of pilot measurements on ecosystem ecology, meteorology, trace gases, and aerosols, *Atmos. Chem. Phys.*, 15(18), 10723–10776, doi:10.5194/acp-15-10723-2015, 2015.
- Bonn, B. and Moortgat, G. K.: Sesquiterpene ozonolysis: Origin of atmospheric new particle formation from biogenic hydrocarbons, *Geophys. Res. Lett.*, 30(11), doi:Artn 1585Doi 10.1029/2003gl017000, 2003.
- Bracho-Nunez, A., Welter, S., Staudt, M. and Kesselmeier, J.: Plant-specific volatile organic compound emission rates from young and mature leaves of Mediterranean vegetation, *J. Geophys. Res.*, 116(D16), D16304, doi:10.1029/2010JD015521, 2011.
- Bracho-Nunez, A., Knothe, N. M., Welter, S., Staudt, M., Costa, W. R., Liberato, M. A. R., Piedade, M. T. F. and Kesselmeier, J.: Leaf level emissions of volatile organic compounds (VOC) from some Amazonian and Mediterranean plants, *Biogeosciences*, 10(9), 5855–5873, doi:10.5194/bg-10-5855-2013, 2013.
- Claeys, M., Graham, B., Vas, G., Wang, W., Vermeylen, R., Pashynska, V., Cafmeyer, J., Guyon, P., Andreae, M. O., Artaxo, P. and Maenhaut, W.: Formation of secondary organic aerosols through photooxidation of isoprene., *Science*, 303(5661), 1173–6, doi:10.1126/science.1092805, 2004.
- Eddingsaas, N. C., Loza, C. L., Yee, L. D., Seinfeld, J. H. and Wennberg, P. O.:  $\alpha$ -pinene photooxidation under controlled chemical conditions – Part 1: Gas-phase composition in low- and high-NO<sub>x</sub> environments, *Atmos. Chem. Phys.*, 12(14), 6489–6504, doi:10.5194/acp-12-6489-2012, 2012.
- Ehn, M., Thornton, J. A., Kleist, E., Sipilä, M., Junninen, H., Pullinen, I., Springer, M., Rubach, F., Tillmann, R., Lee, B., Lopez-Hilfiker, F., Andres, S., Acir, I.-H., Rissanen, M., Jokinen, T., Schobesberger, S., Kangasluoma, J., Kontkanen, J., Nieminen, T., Kurtén, T., Nielsen, L. B., Jørgensen, S., Kjaergaard, H. G., Canagaratna, M., Maso, M. D., Berndt, T., Petäjä, T., Wahner, A., Kerminen, V.-M., Kulmala, M., Worsnop, D. R., Wildt, J. and Mentel, T. F.: A large source of low-volatility secondary organic aerosol., *Nature*, 506(7489), 476–9, doi:10.1038/nature13032, 2014.
- Engelhart, G. J., Asa-Awuku, A., Nenes, A. and Pandis, S. N.: CCN activity and droplet growth kinetics of fresh and aged monoterpene secondary organic aerosol, *Atmos. Chem. Phys.*, 8(14), 3937–3949, doi:10.5194/acp-8-3937-2008, 2008.
- Fry, J. L., Draper, D. C., Barsanti, K. C., Smith, J. N., Ortega, J., Winkler, P. M., Lawler, M. J., Brown, S. S., Edwards, P. M., Cohen, R. C. and Lee, L.: Secondary Organic Aerosol Formation and Organic Nitrate Yield from NO<sub>3</sub> Oxidation of Biogenic Hydrocarbons, *Environ. Sci. Technol.*, 48(20),

11944–11953, doi:10.1021/es502204x, 2014.

574 Ganzeveld, L. and Lelieveld, J.: Impact of Amazonian deforestation on atmospheric chemistry, *Geophys. Res. Lett.*, 31(6), n/a-n/a,  
575 doi:10.1029/2003GL019205, 2004.

576 Ganzeveld, L., Eerdeken, G., Feig, G., Fischer, H., Harder, H., Konigstedt, R., Kubistin, D., Martinez, M., Meixner, F. X., Scheeren, H. A., Sinha, V.,  
577 Taraborrelli, D., Williams, J., de Arellano, J. V. G. and Lelieveld, J.: Surface and boundary layer exchanges of volatile organic compounds,  
578 nitrogen oxides and ozone during the GABRIEL campaign, *Atmos. Chem. Phys.*, 8(20), 6223–6243, 2008.

579 Ganzeveld, L. N., Lelieveld, J., Dentener, F. J., Krol, M. C. and Roelofs, G. -J.: Atmosphere-biosphere trace gas exchanges simulated with a single-column  
580 model, *J. Geophys. Res.*, 107(D16), 4297, doi:10.1029/2001JD000684, 2002.

581 Gershenson, J.: Plant volatiles carry both public and private messages, *Proc. Natl. Acad. Sci. U. S. A.*, 104(13), 5257–8, doi:10.1073/pnas.0700906104,  
582 2007.

583 Gershenson, J. and Dudareva, N.: The function of terpene natural products in the natural world, *Nat. Chem. Biol.*, 3(7), 408–414,  
584 doi:10.1038/nchembio.2007.5, 2007.

585 Ghirardo, A., Koch, K., Taipale, R., Zimmer, I. N. A., Schnitzler, J. P. Jör.-P. and Rinne, J.: Determination of de novo and pool emissions of terpenes from  
586 four common boreal/alpine trees by 13 CO<sub>2</sub> labelling and PTR-MS analysis, *Plant. Cell Environ.*, 33(5), 781–792, doi:10.1111/j.1365-  
587 3040.2009.02104.x, 2010.

588 Gratien, A., Johnson, S. N., Ezell, M. J., Dawson, M. L., Bennett, R. and Finlayson-Pitts, B. J.: Surprising Formation of *p*-Cymene in the Oxidation of  $\alpha$ -  
589 Pinene in Air by the Atmospheric Oxidants OH, O<sub>3</sub>, and NO<sub>3</sub>, *Environ. Sci. Technol.*, 45(7), 2755–2760, doi:10.1021/es103632b, 2011.

590 Greenberg, J. P. and Zimmerman, P. R.: Nonmethane hydrocarbons in remote tropical, continental, and marine atmospheres, *J. Geophys. Res.*, 89(D3),  
591 4767, doi:10.1029/JD089iD03p04767, 1984.

592 Griffin, R. J., Cocker, D. R., Flagan, R. C. and Seinfeld, J. H.: Organic aerosol formation from the oxidation of biogenic hydrocarbons, *J. Geophys. Res.*,  
593 104(D3), 3555–3567, 1999.

594 Guenther, A., Karl, T., Harley, P., Wiedinmyer, C., Palmer, P. I. and Geron, C.: Estimates of global terrestrial isoprene emissions using MEGAN (Model of  
595 Emissions of Gases and Aerosols from Nature), *Atmos. Chem. Phys.*, 6(11), 3181–3210, doi:10.5194/acp-6-3181-2006, 2006.

596 Guenther, A. B., Jiang, X., Heald, C. L., Sakulyanontvittaya, T., Duhl, T., Emmons, L. K. and Wang, X.: The Model of Emissions of Gases and Aerosols  
597 from Nature version 2.1 (MEGAN2.1): an extended and updated framework for modeling biogenic emissions, *Geosci. Model Dev.*, 5(6), 1471–  
598 1492, doi:10.5194/gmd-5-1471-2012, 2012.

599 Hallquist, M., Wenger, J. C., Baltensperger, U., Rudich, Y., Simpson, D., Claeys, M., Dommen, J., Donahue, N. M., George, C., Goldstein, A. H.,  
600 Hamilton, J. F., Herrmann, H., Hoffmann, T., Iinuma, Y., Jang, M., Jenkin, M. E., Jimenez, J. L., Kiendler-Scharr, A., Maenhaut, W., McFiggans,  
601 G., Mentel, T. F., Monod, A., Prévôt, A. S. H., Seinfeld, J. H., Surratt, J. D., Szmigielski, R. and Wildt, J.: The formation, properties and impact of  
602 secondary organic aerosol: current and emerging issues, *Atmos. Chem. Phys.*, 9(14), 5155–5236, doi:10.5194/acp-9-5155-2009, 2009.

603 Hatakeyama, S., Izumi, K., Fukuyama, T. and Akimoto, H.: Reactions of ozone with  $\alpha$ -pinene and  $\beta$ -pinene in air: Yields of gaseous and particulate  
604 products, *J. Geophys. Res.*, 94(D10), 13013, doi:10.1029/JD094iD10p13013, 1989.

605 Helmig, D., Greenberg, J., Guenther, A., Zimmerman, P. and Geron, C.: Volatile organic compounds and isoprene oxidation products at a temperate  
606 deciduous forest site, *J. Geophys. Res.*, 103(D17), 22397, doi:10.1029/98JD00969, 1998.

607 Herrmann, F., Winterhalter, R., Moortgat, G. K. and Williams, J.: Hydroxyl radical (OH) yields from the ozonolysis of both double bonds for five  
608 monoterpenes, *Atmos. Environ.*, 44(28), 3458–3464, doi:10.1016/j.atmosenv.2010.05.011, 2010.

609 Hoffmann, T., Odum, J. R., Bowman, F., Collins, D., Klockow, D., Flagan, R. C. and Seinfeld, J. H.: Formation of Organic Aerosols from the Oxidation of  
610 Biogenic Hydrocarbons, *J. Atmos. Chem.*, 26(2), 189–222, doi:10.1023/a:1005734301837, 1997.

611 Jardine, A. B., Jardine, K. J., Fuentes, J. D., Martin, S. T., Martins, G., Durgante, F., Carneiro, V., Higuchi, N., Manzi, A. O. and Chambers, J. Q.: Highly  
612 reactive light-dependent monoterpenes in the Amazon, *Geophys. Res. Lett.*, 42(5), 1576–1583, doi:10.1002/2014GL062573, 2015.

613 Jardine, K., Yañez Serrano, A., Arneth, A., Abrell, L., Jardine, A., van Haren, J., Artaxo, P., Rizzo, L. V., Ishida, F. Y., Karl, T., Kesselmeier, J., Saleska, S.  
614 and Huxman, T.: Within-canopy sesquiterpene ozonolysis in Amazonia, *J. Geophys. Res.*, 116(D19), D19301, doi:10.1029/2011JD016243, 2011.

615 Jardine, K. J., Jardine, A. B., Holm, J. A., Lombardozi, D. L., Negron-Juarez, R. I., Martin, S. T., Beller, H. R., Gimenez, B. O., Higuchi, N. and  
616 Chambers, J. Q.: Monoterpene “*thermometer*” of tropical forest-atmosphere response to climate warming, *Plant. Cell Environ.*, 40(3), 441–452,  
617 doi:10.1111/pce.12879, 2017.

618 Jokinen, T., Berndt, T., Makkonen, R., Kerminen, V.-M., Junninen, H., Paasonen, P., Stratmann, F., Herrmann, H., Guenther, A. B., Worsnop, D. R.,  
619 Kulmala, M., Ehn, M. and Sipilä, M.: Production of extremely low volatile organic compounds from biogenic emissions: Measured yields and  
620 atmospheric implications, *Proc. Natl. Acad. Sci. U. S. A.*, 112(23), 7123–8, doi:10.1073/pnas.1423977112, 2015.

621 Karl, T., Guenther, A., Yokelson, R. J., Greenberg, J., Potosnak, M., Blake, D. R. and Artaxo, P.: The tropical forest and fire emissions experiment:  
622 Emission, chemistry, and transport of biogenic volatile organic compounds in the lower atmosphere over Amazonia, *J. Geophys. Res.*, 112(D18),  
623 D18302, doi:10.1029/2007JD008539, 2007.

624 Kesselmeier, J. and Staudt, M.: Biogenic volatile organic compounds (VOC): An overview on emission, physiology and ecology, *J. Atmos. Chem.*, 33(1),  
625 23–88, doi:10.1023/A:1006127516791, 1999.

626 Kesselmeier, J., Kuhn, U., Rottenberger, S., Biesenthal, T., Wolf, A., Schebeske, G., Andreae, M. O., Ciccioli, P., Brancaleoni, E., Frattoni, M., Oliva, S. T.,  
627 Botelho, M. L., Silva, C. M. A. and Tavares, T. M.: Concentrations and species composition of atmospheric volatile organic compounds (VOCs) as  
628 observed during the wet and dry season in Rondonia (Amazonia), *J. Geophys. Res.*, 107(D20), 1–13, doi:10.1029/2000jd000267, 2002.

629 Kiendler-Scharr, A., Wildt, J., Dal Maso, M., Hohaus, T., Kleist, E., Mentel, T. F., Tillmann, R., Uerlings, R., Schurr, U. and Wahner, A.: New particle  
630 formation in forests inhibited by isoprene emissions, *Nature*, 461(7262), 381–4, doi:10.1038/nature08292, 2009.

631 Kishimoto, K., Matsui, K., Ozawa, R. and Takabayashi, J.: Analysis of defensive responses activated by volatile allo-ocimene treatment in *Arabidopsis*  
632 *thaliana*, *Phytochemistry*, 67(14), 1520–1529, doi:10.1016/j.phytochem.2006.05.027, 2006.

633 Komenda, M.: Investigations of the emissions of monoterpenes from Scots pine, *Universität Köln, Jülich*, 2001.

634 Kuhn, U., Rottenberger, S., Biesenthal, T., Wolf, A., Schebeske, G., Ciccioli, P., Brancaleoni, E., Frattoni, M., Tavares, T. M. and Kesselmeier, J.: Isoprene  
635 and monoterpene emissions of Amazonian tree species during the wet season: Direct and indirect investigations on controlling environmental

636 functions, *J. Geophys. Res.*, 107(D20), doi:807110.1029/2001jd000978, 2002.

637 Kuhn, U., Rottenberger, S., Biesenthal, T., Wolf, A., Schebeske, G., Ciccioli, P., Brancaleoni, E., Frattoni, M., Tavares, T. M. and Kesselmeier, J.: Seasonal  
638 differences in isoprene and light-dependent monoterpene emission by Amazonian tree species, *Glob. Chang. Biol.*, 10(5), 663–682,  
639 doi:10.1111/j.1529-8817.2003.00771.x, 2004.

640 Kuhn, U., Dindorf, T., Ammann, C., Rottenberger, S., Guyon, P., Holzinger, R., Ausma, S., Kenntner, T., Helleis, F. and Kesselmeier, J.: Design and field  
641 application of an automated cartridge sampler for VOC concentration and flux measurements., *J. Environ. Monit.*, 7(6), 568–76,  
642 doi:10.1039/b500057b, 2005.

643 Kuhn, U., Ganzeveld, L., Thielmann, A., Dindorf, T., Schebeske, G., Welling, M., Sciare, J., Roberts, G., Meixner, F. X., Kesselmeier, J., Lelieveld, J.,  
644 Kolle, O., Ciccioli, P., Lloyd, J., Trentmann, J., Artaxo, P. and Andreae, M. O.: Impact of Manaus City on the Amazon Green Ocean atmosphere:  
645 ozone production, precursor sensitivity and aerosol load, *Atmos. Chem. Phys.*, 10(19), 9251–9282, doi:10.5194/acp-10-9251-2010, 2010.

646 Lammel, G.: Formation of nitrous acid parameterisation and comparison with observations, Max-Planck-Inst. für Meteorologie, Hamburg., 1999.

647 Lerda, M., Litvak, M., Palmer, P. and Monson, R.: Controls over monoterpene emissions from boreal forest conifers, *Tree Physiol.*, 17(8–9), 563–569,  
648 doi:10.1093/treephys/17.8-9.563, 1997.

649 Lichtenthaler, H. K.: The 1-deoxy-d-xylulose-5-phosphate pathway of isoprenoid biosynthesis in plants, *Annu. Rev. Plant Physiol. Plant Mol. Biol.*, 50(1),  
650 47–65, doi:10.1146/annurev.arplant.50.1.47, 1999.

651 Lopes, A. P., Nelson, B. W., Wu, J., Graça, P. M. L. de A., Tavares, J. V., Prohaska, N., Martins, G. A. and Saleska, S. R.: Leaf flush drives dry season  
652 green-up of the Central Amazon, *Remote Sens. Environ.*, 182, 90–98, doi:10.1016/j.rse.2016.05.009, 2016.

653 Maag, D., Erb, M., Köllner, T. G. and Gershenzon, J.: Defensive weapons and defense signals in plants: Some metabolites serve both roles, *BioEssays*,  
654 37(2), 167–174, doi:10.1002/bies.201400124, 2015.

655 Malhi, Y., Roberts, J. T., Betts, R. A., Killeen, T. J., Li, W. H. and Nobre, C. A.: Climate change, deforestation, and the fate of the Amazon, *Science (80-. )*,  
656 319(5860), 169–172, doi:10.1126/science.1146961, 2008.

657 Martin, S. T., Andreae, M. O., Artaxo, P., Baumgardner, D., Chen, Q., Goldstein, A. H., Guenther, A., Heald, C. L., Mayol-Bracero, O. L., McMurry, P. H.,  
658 Pauliquevis, T., Poschl, U., Prather, K. A., Roberts, G. C., Saleska, S. R., Dias, M. A. S., Spracklen, D. V., Swietlicki, E., Trebs, I., Bracero, O. L.  
659 M. and Pöschl, U.: Sources and properties of amazonian aerosol particles, *Rev. Geophys.*, 48(2008), doi:Rg200210.1029/2008rg000280, 2010.

660 Mentel, T. F., Wildt, J., Kiendler-Scharr, A., Kleist, E., Tillmann, R., Dal Maso, M., Fisseha, R., Hohaus, T., Spahn, H., Uerlings, R., Wegener, R.,  
661 Griffiths, P. T., Dinar, E., Rudich, Y. and Wahner, A.: Photochemical production of aerosols from real plant emissions, *Atmos. Chem. Phys.*, 9(13),  
662 4387–4406, doi:10.5194/acp-9-4387-2009, 2009.

663 Neeb, P., Bode, K., Beck, J., Schafer, L., Kesselmeier, J. and Moortgat: Influence of gas-phase oxidation on estimated emission rates of biogenic  
664 hydrocarbons, in *The Oxidizing Capacity of the Atmosphere, Proceedings Physico-Chemical, of the 7th European Symposium on the Behaviour of*  
665 *Atmospheric Pollutants, EUR 17482.*, edited by B. Larsen, B. Versino, and G. Angeletti, p. 295±299, Office for Official Publications of the  
666 European Communities, Brussels, Belgium., 1997.

667 Nölscher, A. C., Yañez-Serrano, A. M., Wolff, S., de Araujo, A. C., Lavrić, J. V., Kesselmeier, J. and Williams, J.: Unexpected seasonality in quantity and  
668 composition of Amazon rainforest air reactivity, *Nat. Commun.*, 7, 10383, doi:10.1038/ncomms10383, 2016.

669 O'Dowd, C. D., Aalto, P., Hameri, K., Kulmala, M. and Hoffmann, T.: Aerosol formation - Atmospheric particles from organic vapours, *Nature*, 416(6880),  
670 497–498, 2002.

671 Ormeno, E., Fernandez, C., Bousquet-Melou, A., Greff, S., Morin, E., Robles, C., Vila, B. and Bonin, G.: Monoterpene and sesquiterpene emissions of three  
672 Mediterranean species through calcareous and siliceous soils in natural conditions, *Atmos. Environ.*, 41(3), 629–639,  
673 doi:10.1016/j.atmosenv.2006.08.027, 2007.

674 Paulson, S. E., Chung, M. Y. and Hanson, A. S.: OH Radical Formation from the Gas-Phase Reaction of Ozone with Terminal Alkenes and the Relationship  
675 between Structure and Mechanism, *J. Phys. Chem. A*, 103(41), 8125–8138, doi:10.1021/jp991995e, 1999.

676 Penuelas, J. and Llusia, J.: Linking photorespiration, monoterpenes and thermotolerance in Quercus, *New Phytol.*, 155(2), 227–237, doi:10.1046/j.1469-  
677 8137.2002.00457.x, 2002.

678 Pöschl, U., Martin, S. T., Sinha, B., Chen, Q., Gunthe, S. S., Huffman, J. A., Borrmann, S., Farmer, D. K., Garland, R. M., Helas, G., Jimenez, J. L., King,  
679 S. M., Manzi, A., Mikhailov, E., Pauliquevis, T., Petters, M. D., Prenni, A. J., Roldin, P., Rose, D., Schneider, J., Su, H., Zorn, S. R., Artaxo, P.,  
680 Andreae, M. O., Poschl, U., Martin, S. T., Sinha, B., Chen, Q., Gunthe, S. S., Huffman, J. A., Borrmann, S., Farmer, D. K., Garland, R. M., Helas,  
681 G., Jimenez, J. L., King, S. M., Manzi, A., Mikhailov, E., Pauliquevis, T., Petters, M. D., Prenni, A. J., Roldin, P., Rose, D., Schneider, J., Su, H.,  
682 Zorn, S. R., Artaxo, P. and Andreae, M. O.: Rainforest Aerosols as Biogenic Nuclei of Clouds and Precipitation in the Amazon, *Science (80-. )*,  
683 329(5998), 1513–1516, doi:10.1126/science.1191056, 2010.

684 Rinne, H. J. L., Guenther, A. B., Greenberg, J. P. and Harley, P. C.: Isoprene and monoterpene fluxes measured above Amazonian rainforest and their  
685 dependence on light and temperature, *Atmos. Environ.*, 36(14), 2421–2426, doi:10.1016/S1352-2310(01)00523-4, 2002.

686 Sarrafzadeh, M., Wildt, J., Pullinen, I., Springer, M., Kleist, E., Tillmann, R., Schmitt, S. H., Wu, C., Mentel, T. F., Zhao, D., Hastie, D. R. and Kiendler-  
687 Scharr, A.: Impact of NOx and OH on secondary organic aerosol formation from  $\beta$ -pinene photooxidation, *Atmos. Chem. Phys.*, 16(17), 11237–  
688 11248, doi:10.5194/acp-16-11237-2016, 2016.

689 Schwender, J., Seemann, M., Lichtenthaler, H. K. and Rohmer, M.: Biosynthesis of isoprenoids (carotenoids, sterols, prenyl side-chains of chlorophylls and  
690 plastoquinone) via a novel pyruvate/glyceraldehyde 3-phosphate non-mevalonate pathway in the green alga *Scenedesmus obliquus*, *Biochem. J.*,  
691 316(1), 73–80, doi:10.1042/bj3160073, 1996.

692 Spivakovskiy, C. A. M., Logan, J. A., Montzka, S. A., Balkanski, Y. J., Foreman-Fowler, M., Jones, D. B. A., Horowitz, L. W., Fusco, A. C., Brenninkmeijer,  
693 C. A. M., Prather, M. J., Wofsy, S. C. and McElroy, M. B.: Three-dimensional climatological distribution of tropospheric OH: Update and  
694 evaluation, *J. Geophys. Res. Atmos.*, 105(D7), 8931–8980, doi:10.1029/1999JD901006, 2000.

695 Sternberg, J. C., Galloway, W. S. and Jones, D. T. L.: The mechanism of response of flame ionisation detectors, in *Gas Chromatography*, edited by N.  
696 Brenner, J. E. Callin, and M. D. Weiss, Academic press, New York., 1962.

697 Sun, S., Moravek, A., von der Heyden, L., Held, A., Sörgel, M. and Kesselmeier, J.: Twin-cuvette measurement technique for investigation of dry  
698 deposition of O<sub>3</sub> and PAN to plant leaves under controlled humidity conditions, *Atmos. Meas. Tech.*, 9(2), 599–617, doi:10.5194/amt-9-599-2016,

- 699 2016.
- 700 Vickers, C. E., Gershenzon, J., Lerdau, M. T. and Loreto, F.: A unified mechanism of action for volatile isoprenoids in plant abiotic stress, *Nat. Chem.*
- 701 *Biol.*, 5(5), 283–291, doi:10.1038/nchembio.158, 2009.
- 702 Wesely, M. L.: Parameterization of surface resistances to gaseous dry deposition in regional-scale numerical models, *Atmos. Environ.*, 23(6), 1293–1304,
- 703 doi:10.1016/0004-6981(89)90153-4, 1989.
- 704 Wildt, J., Mentel, T. F., Kiendler-Scharr, A., Hoffmann, T., Andres, S., Ehn, M., Kleist, E., M $\ddot{u}$ sgen, P., Rohrer, F., Rudich, Y., Springer, M., Tillmann, R.
- 705 and Wahner, A.: Suppression of new particle formation from monoterpene oxidation by NO $_x$ , *Atmos. Chem. Phys.*, 14(6), 2789–2804,
- 706 doi:10.5194/acp-14-2789-2014, 2014.
- 707 Williams, J., Yassaa, N., Bartenbach, S. and Lelieveld, J.: Mirror image hydrocarbons from Tropical and Boreal forests, *Atmos. Chem. Phys.*, 7(3), 973–
- 708 980, doi:10.5194/acp-7-973-2007, 2007.
- 709 Williams, J., Keßel, S. U., Nölscher, A. C., Yang, Y., Lee, Y., Yáñez-Serrano, A. M., Wolff, S., Kesselmeier, J., Klüpfel, T., Lelieveld, J. and Shao, M.:  
710 Opposite OH reactivity and ozone cycles in the Amazon rainforest and megacity Beijing: Subversion of biospheric oxidant control by  
711 anthropogenic emissions, *Atmos. Environ.*, 125, 112–118, doi:10.1016/j.atmosenv.2015.11.007, 2016.
- 712 Wu, J., Albert, L. P., Lopes, A. P., Restrepo-Coupe, N., Hayek, M., Wiedemann, K. T., Guan, K., Stark, S. C., Christoffersen, B., Prohaska, N., Tavares, J.
- 713 V., Marostica, S., Kobayashi, H., Ferreira, M. L., Campos, K. S., da Silva, R., Brando, P. M., Dye, D. G., Huxman, T. E., Huete, A. R., Nelson, B.
- 714 W. and Saleska, S. R.: Leaf development and demography explain photosynthetic seasonality in Amazon evergreen forests, *Science* (80-. ),
- 715 351(6276), 972–976, doi:10.1126/science.aad5068, 2016.
- 716 Yáñez-Serrano, A. M., Nölscher, A. C., Williams, J., Wolff, S., Alves, E. G., Martins, G. A., Boutsoukidis, E., Brito, J., Jardine, K., Artaxo, P. and  
717 Kesselmeier, J.: Diel and seasonal changes of biogenic volatile organic compounds within and above an Amazonian rainforest, *Atmos. Chem.*  
718 *Phys.*, 15(6), 3359–3378, doi:10.5194/acp-15-3359-2015, 2015.
- 719 Zhao, D. F., Kaminski, M., Schlag, P., Fuchs, H., Acir, I.-H., Bohn, B., Häsel, R., Kiendler-Scharr, A., Rohrer, F., Tillmann, R., Wang, M. J., Wegener,  
720 R., Wildt, J., Wahner, A. and Mentel, T. F.: Secondary organic aerosol formation from hydroxyl radical oxidation and ozonolysis of monoterpenes,  
721 *Atmos. Chem. Phys.*, 15(2), 991–1012, doi:10.5194/acp-15-991-2015, 2015.
- 722 Zhou, P., Ganzeveld, L., Taipale, D., Rannik, Ü., Rantala, P., Rissanen, M. P., Chen, D. and Boy, M.: Boreal forest BVOC exchange: emissions versus in-  
723 canopy sinks, *Atmos. Chem. Phys.*, 17(23), 14309–14332, doi:10.5194/acp-17-14309-2017, 2017.

724

725 Table 1: Average mixing ratio with standard deviation in ppb at 24 and 12 m of the measured monoter-  
726 pene species from 17 to 20 October 2015 as determined by the GC-FID analysis. The daytime period  
727 was chosen from 0900h to 1700h and the night time period from 2000h to 0500h (Local time). BLD  
728 stands for below detection limit.

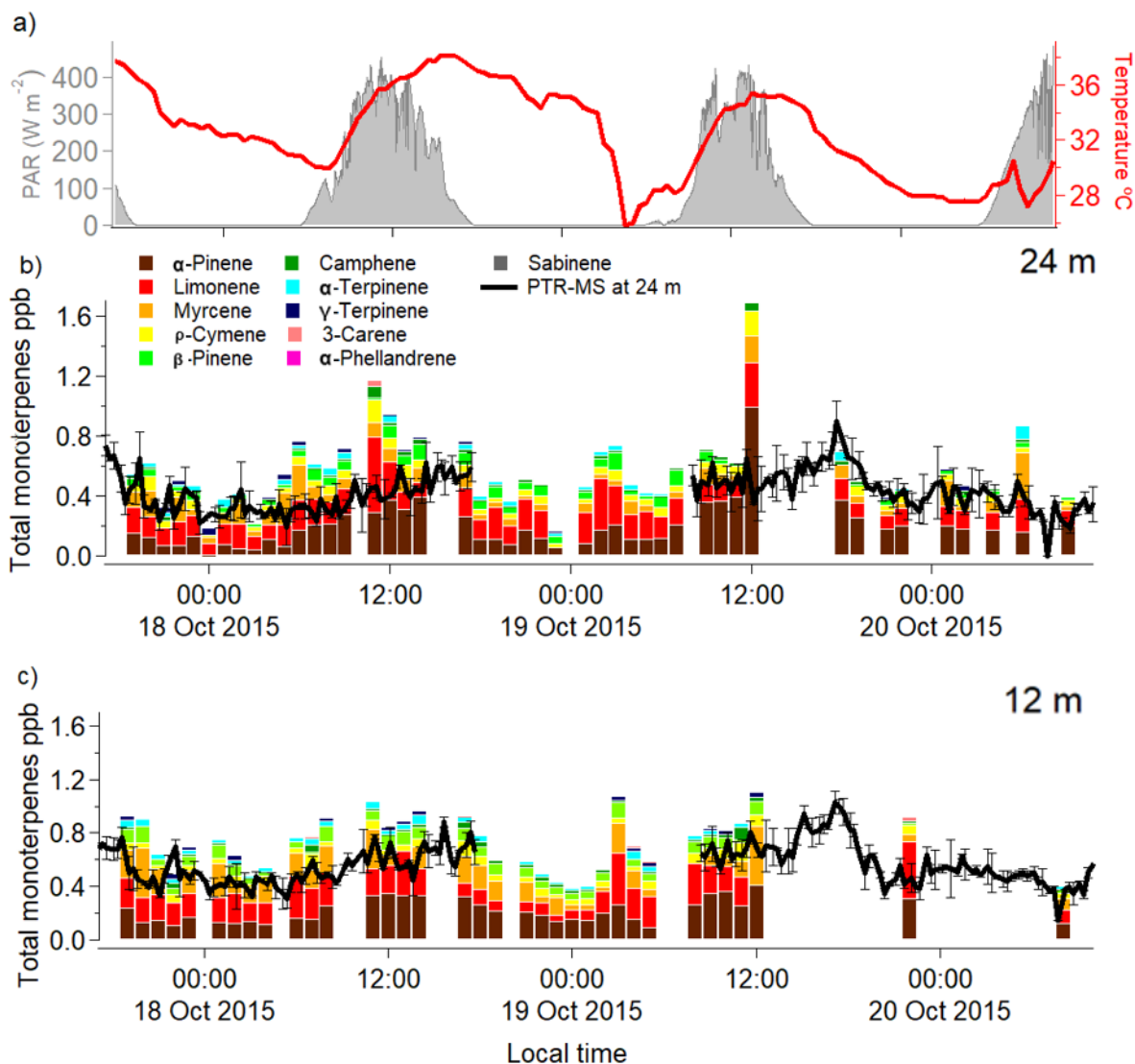
Compound	Day 12 m	Night 12 m	Day 24 m	Night 24 m
$\alpha$ -Pinene	0.33 $\pm$ 0.04	0.15 $\pm$ 0.05	0.38 $\pm$ 0.21	0.11 $\pm$ 0.06
Limonene	0.18 $\pm$ 0.09	0.18 $\pm$ 0.10	0.19 $\pm$ 0.12	0.14 $\pm$ 0.07
Myrcene	0.16 $\pm$ 0.14	0.12 $\pm$ 0.09	0.09 $\pm$ 0.04	0.07 $\pm$ 0.06
P-Cymene	0.07 $\pm$ 0.03	0.04 $\pm$ 0.01	0.08 $\pm$ 0.04	0.04 $\pm$ 0.02
$\beta$ -Pinene	0.08 $\pm$ 0.03	0.06 $\pm$ 0.03	0.05 $\pm$ 0.03	0.04 $\pm$ 0.02
Camphene	0.03 $\pm$ 0.03	0.02 $\pm$ 0.01	0.03 $\pm$ 0.02	0.01 $\pm$ 0.01
$\alpha$ -Terpinene	0.03 $\pm$ 0.02	0.03 $\pm$ 0.02	0.01 $\pm$ 0.02	0.02 $\pm$ 0.02
$\gamma$ -Terpinene	0.02 $\pm$ 0.01	0.01 $\pm$ 0.01	0.01 $\pm$ 0.01	0.01 $\pm$ 0.01
3-Carene	0.001 $\pm$ 0.003	0.003 $\pm$ 0.008	0.003 $\pm$ 0.011	0 or BLD
$\alpha$ -Phellandrene	0 or BLD	0 or BLD	0 or BLD	0 or BLD
Sabinene	0 or BLD	0 or BLD	0 or BLD	0 or BLD
MT Sum – GC-FID	0.91 $\pm$ 0.10	0.62 $\pm$ 0.19	0.82 $\pm$ 0.34	0.45 $\pm$ 0.13
MT Sum – PTR-MS	0.96 $\pm$ 0.27	0.54 $\pm$ 0.17	0.77 $\pm$ 0.22	0.56 $\pm$ 0.16

729

730 Table 2: Lifetime of the different monoterpene species related to OH, O<sub>3</sub> and NO<sub>3</sub> for the OH daytime  
 731 conditions at 24 m and at 12 m. In addition, the normalized reactivity to 1 ppb of the different monoter-  
 732 pene species is calculated.

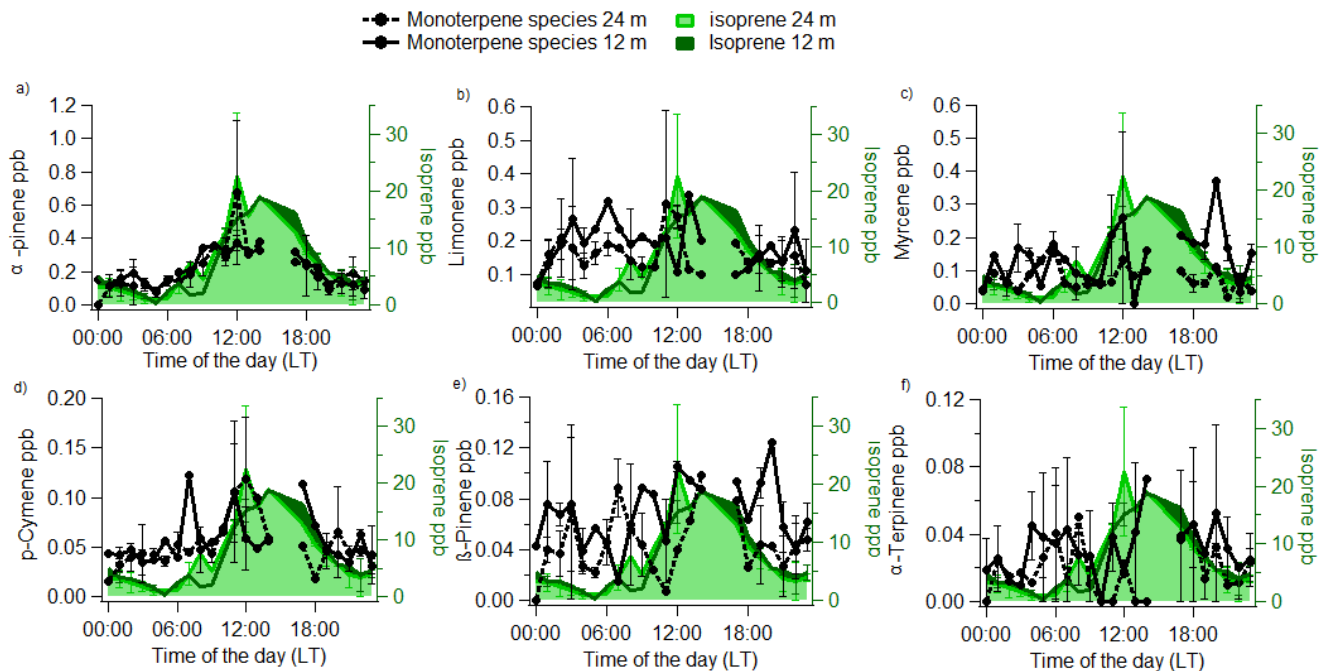
Monoterpenes inves- tigated	Formula	Lifetime (minutes)			Normalized reactivity to 1 ppb s <sup>-1</sup>		
		OH	O <sub>3</sub>	NO <sub>3</sub>	OH	O <sub>3</sub>	NO <sub>3</sub>
α-Pinene	C <sub>10</sub> H <sub>16</sub>	449	615	250	1.42	2.3E-06	0.17
Camphene	C <sub>10</sub> H <sub>16</sub>	447	57422	2461	1.43	2.4E-08	0.02
Sabinene	C <sub>10</sub> H <sub>16</sub>	400	623	155	1.60	2.2E-06	0.27
β-Pinene	C <sub>10</sub> H <sub>16</sub>	320	3445	618	2.00	4.0E-07	0.07
Myrcene	C <sub>10</sub> H <sub>16</sub>	71	110	141	8.98	1.3E-05	0.30
α-Phellandrene	C <sub>10</sub> H <sub>16</sub>	132	17	21	4.84	8.1E-05	1.96
Δ <sup>3</sup> -Carene	C <sub>10</sub> H <sub>16</sub>	271	1397	170	2.37	9.9E-07	0.24
α-Terpinene	C <sub>10</sub> H <sub>16</sub>	103	2	11	6.24	5.6E-04	3.76
ρ-Cymene	C <sub>10</sub> H <sub>14</sub>	1577	>90000	>90000	0.41	1.3E-09	2.7E-05
Limonene	C <sub>10</sub> H <sub>16</sub>	145	246	127	4.41	5.6E-06	0.33
γ-Terpinene	C <sub>10</sub> H <sub>16</sub>	140	369	53	4.57	3.8E-06	0.78
Isoprene	C <sub>5</sub> H <sub>8</sub>	238	4069	238	2.69	3.4E-07	0.02

733



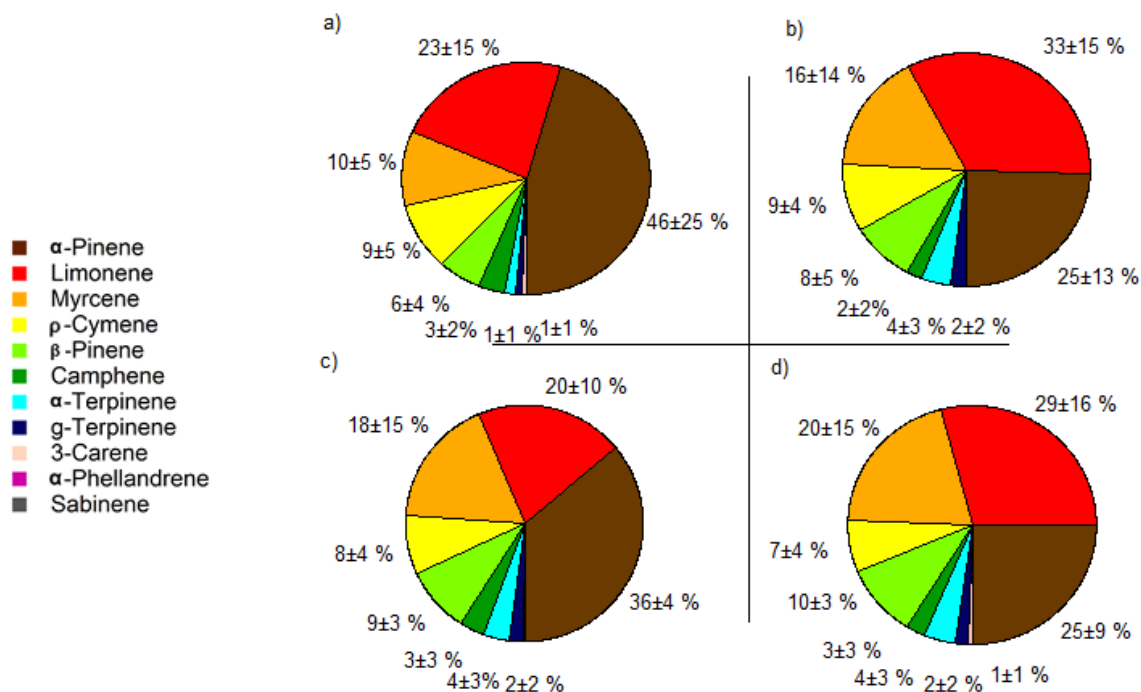
734  
735  
736  
737  
738  
739  
740

Figure 1: Graph showing the speciated monoterpene mixing ratios measured hourly from 17 to 20 October 2015 for 24 m (b) and 12 m (c). The colours on the stacked bar plot indicate the different monoterpene species as they are denoted in the legend. The black line represents the PTR-MS total monoterpene mixing ratio, with a gap of data on the 19 October 2015. Temperature at 80 m is shown as the red thick line and photosynthetically active radiation at 39 m is shown by the shaded areas (a).

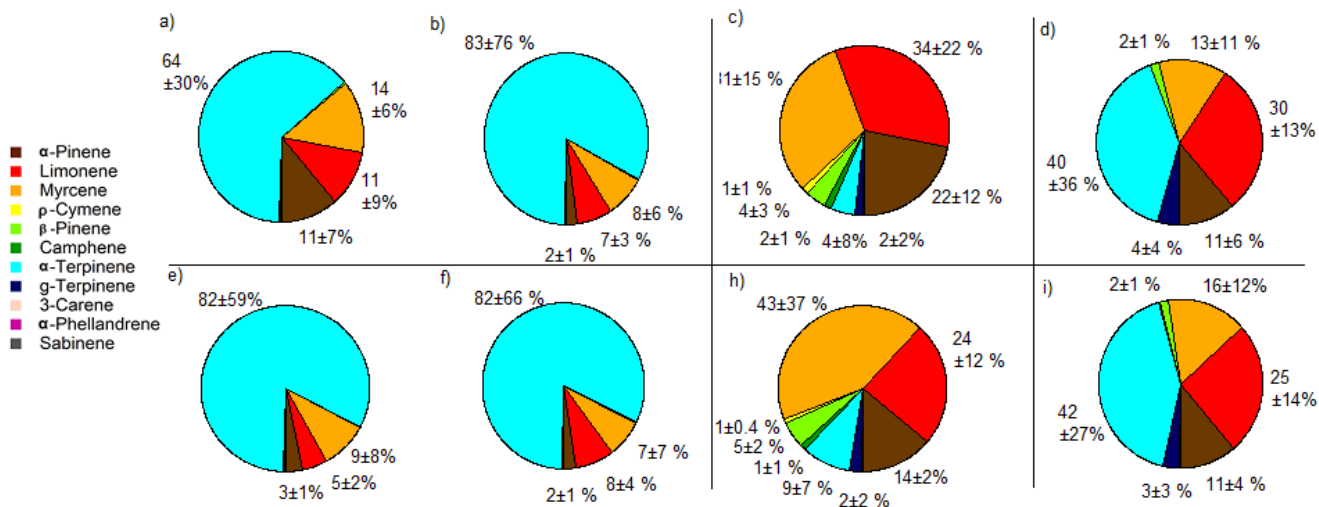


741  
742  
743  
744  
745  
746

Figure 2: Average diel cycles for  $\alpha$ -pinene (a), limonene (b), myrcene (c),  $p$ -cymene (d),  $\beta$ -pinene (e) and  $\alpha$ -terpinene (f) mixing ratios for 24 m (dashed line) and 12 m (thick line). In the back, average diel cycle of isoprene mixing ratios as measured by the GC-FID are shown for 24 m (light green) and 24 m (dark green). Error bars represent the standard deviation of the averages.

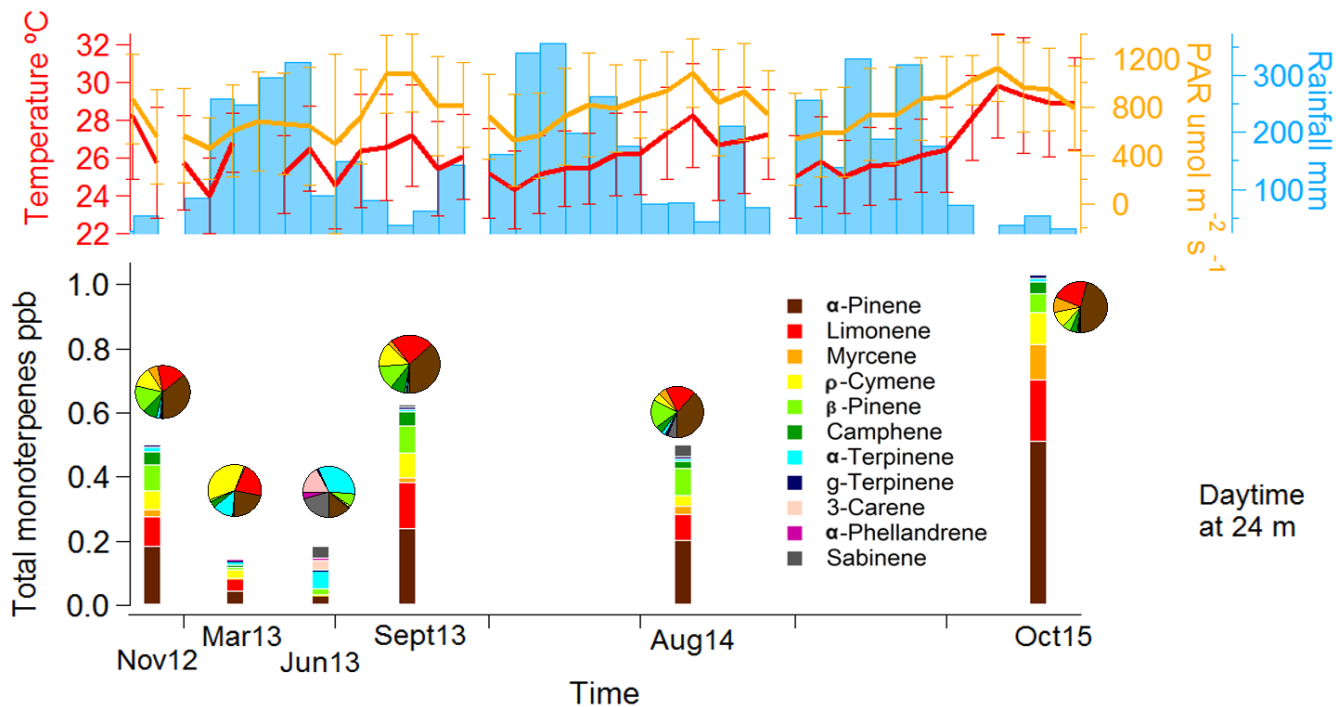


747  
748 Figure 3: Pie charts representing the day (a and c) and night (b and d) average monoterpene species  
749 abundances from 17 to 20 October 2015, with the average percentages and standard deviations at 24 (a  
750 and b) and 12 (c and d) m. The day period was from 0900h to 1700h and the night period was from  
751 2000h to 0500h.  
752

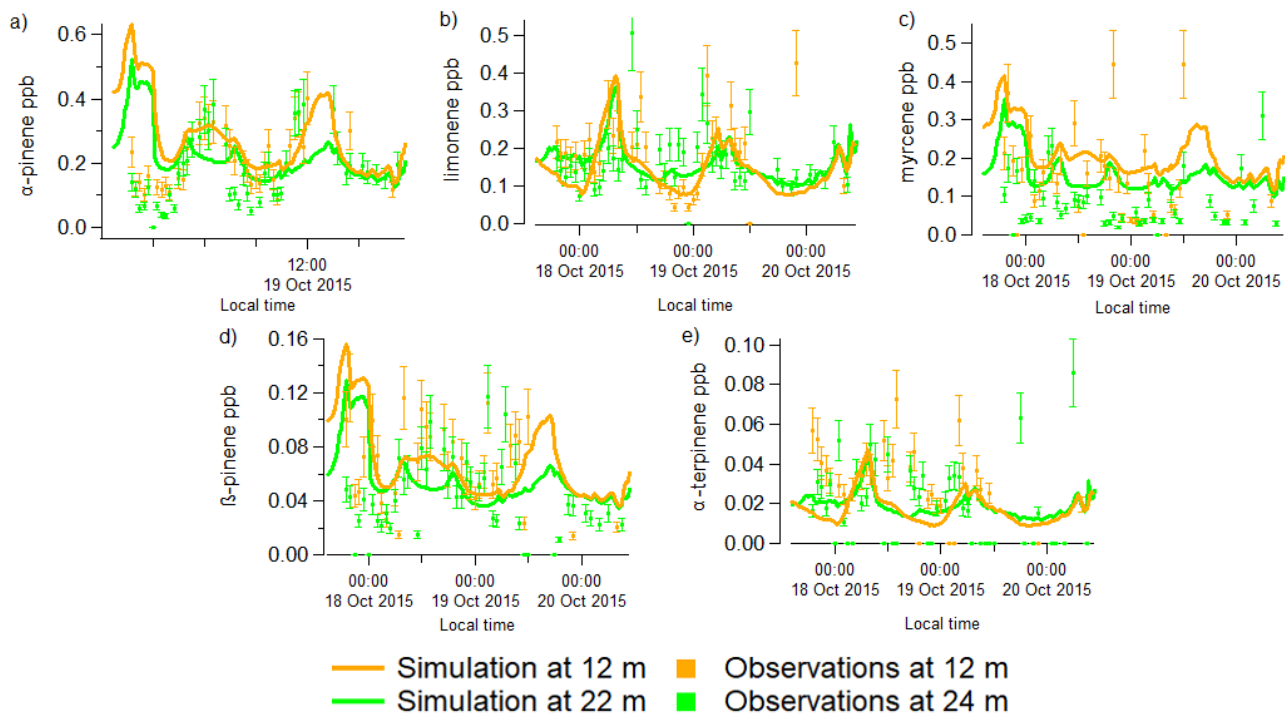


753  
754 Figure 4: Pie charts representing day (a and e) and night (b and f) ozone reactivity, OH reactivity (only  
755 for day, c and h) and NO<sub>3</sub> reactivities from 17 to 20 October 2015, with the average percentages and

756 standard deviations (only for night, d and i), for 12 m on the bottom and 24 m on the top. The day peri-  
 757 od was from 0900h to 1700h and the night period was from 2000h to 0500h.  
 758



759  
 760 Figure 5: Monoterpene mixing ratio chemical speciation during the seasons of measurement. In the top,  
 761 the monthly average of temperature (in red) and photosynthetically active radiation (in orange) are dis-  
 762 played with their standard deviations for the 80 m height. Rain, also on top, is displayed as mm per  
 763 month (bars). At the bottom, the different monoterpene species are differentiated by colours, stacked  
 764 together adding up to the sum of monoterpenes. On top of each bar, a chart pie with the chemical speci-  
 765 ation is shown for easier visualization.



766

767

768

769

770

Figure 6: Comparison between simulated results (solid lines) for 12.5 m (orange) and 22.5 m (green) from MLC-CHEM, with the GC-FID speciated mixing ratios measurements (in ppb) for  $\alpha$ -pinene (a), limonene (b), myrcene (c),  $\beta$ -pinene (d) and  $\alpha$ -terpinene (e) at ATTO from 17 to 20 October 2015. The error bars represent the 20% uncertainty involved in the GC-FID measurements.